Transactions, SMiRT-22
San Francisco, California, USA - August 18-23, 2013
Division X

PRELIMINARY INVESTIGATION OF JOINT SHEAR STRENGTH OF SC WALL-TO-WALL T-JOINTS

Jungil Seo[1], Amit Varma[2], Derek Winkler[3]

[1] Ph. D. Candidate, Purdue University, West Lafayette, IN
[2] Assoc. Prof., Dept. of Civil Engineering, Purdue University, West Lafayette, IN (ahvarma@purdue.edu)
[3] Structural Engineer, URS Corporation, Denver, CO

ABSTRACT

Analytical and experimental studies were conducted to investigate the joint shear behavior and strength of steel-plate composite (SC) wall-to-wall T-joints in safety-related nuclear facilities. This paper focuses on T-joints, which occur commonly in containment internal structures and other similar structures. Full-strength connection design is recommended for such wall-to-wall T-joints, where energy dissipation occurs through inelasticity and formation of plastic hinges in the SC walls, and the joint region has adequate shear strength to resist the demands placed on it by the plastic hinges in the connected SC walls. Since joint shear strength is the focus of this paper, experimental and analytical studies were conducted on specimens designed to fail in shear in the joint region. A large-scale test was conducted on an SC wall-to-wall T-joint specimen that was designed to fail in joint shear. A detailed nonlinear finite element model was developed to predict the behavior of the tested specimen, and to gain additional insights into the observed behavior. The experimental and analytical results are compared with ACI 349-06 code provisions for calculating the joint shear strength of reinforced concrete beam-to-column joints.

INTRODUCTION

Steel-plate composite (SC) structures have been used for the primary and secondary shield walls within the containment internal structures (CIS) of the third generation nuclear power plants. They are also being considered for the small modular reactors (SMR). Significant research has been conducted on the behavior, analysis, and design of SC walls in the US and abroad (KEPIC-SNG 2010 and Varma et al. 2011). Design recommendations have been developed based on findings from the investigations.

The joint regions of SC walls are typically designed such that the connection strength is greater than that of the connected SC walls. In addition, the connected SC walls are detailed to undergo inelastic deformations and have adequate ductility. In order to design the joint regions of SC walls properly, it is important to estimate the strength of the joint region and confirm that the corresponding expected strength of the connected SC walls is smaller than that of the joint regions.

Research on the behavior and design of SC wall-to-wall joints is somewhat limited. In this study, the fundamental behavior and design of SC wall-to-wall joints was investigated experimentally and analytically. The objectives of this study were to (i) evaluate the joint shear behavior of SC wall-to-wall joints analytically and experimentally and (ii) confirm that the joint shear strength equation given in ACI 349-06 Section 21.5.3 is applicable to SC wall-to-wall joints.

SC walls consist of thick concrete walls with steel faceplates (typically 0.375 - 1.0 in. thick) on the exterior surfaces acting as reinforcement. The steel faceplates are made from A36 or A572 Gr. 50 steel and anchored to the concrete infill (typically f'_c = 4000 - 6000 psi) using steel headed shear studs. Steel headed shear studs are placed close enough to prevent local buckling of steel faceplates. The exterior steel faceplates are connected to each other through the concrete using tie bars in the form of structural elements such as angles, channels, steel plates.

One of the most common joint configurations of SC wall-to-wall joints in containment internal structures of the third generation nuclear power plants is the T joint illustrated in Figure 1. The joint

regions are divided from connected SC walls with steel diaphragm plates, and detailed with steel headed shear studs and tie bars such as angles, channels, and steel plates.

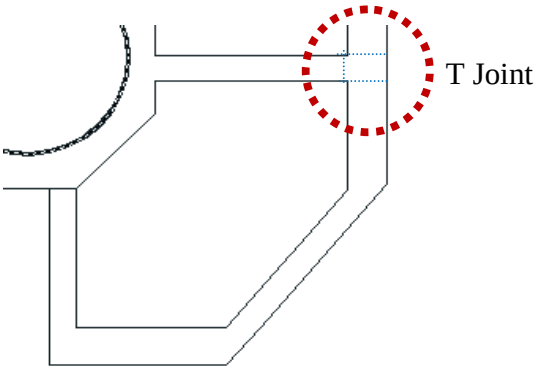

Figure 1 Typical T joint configuration in CIS

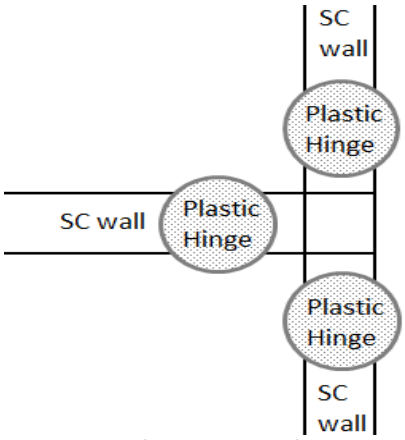

Figure 2 – Recommended failure mode for T-joints

JOINT SHEAR STRENGTH AND ACI 349-06

Full-strength connection design is recommended for such wall-to-wall T-joints, where energy dissipation occurs through inelasticity and formation of plastic hinges in the SC walls as shown in Figure 2, and the joint region has adequate shear strength to resist the demands placed on it by the plastic hinges in the connected SC walls and the yielded steel plates of the SC walls. However, currently there is limited information on the joint shear behavior and strength of SC wall T-joints. In the absence of better information, the joint shear strength of reinforced concrete (RC) beam-to-column joints was considered for the SC wall T-joints.

The strength of reinforced concrete beam-column joints is estimated using Equation (1), which is given in ACI 349-06 Section 21.5.3. The value of γ in the equation is given in Section 21.5.3 of ACI 349-06. It is adopted from ACI 352R-02, which recommends γ values for RC beam-column joints with various configurations. The γ value of 12 for RC beam-column joints (Case A and Type B in ACI 352R-02) with one column framing into the joint was selected for SC wall-to-wall T joints. The effective cross-sectional area within a joint (A_j) is calculated using the effective joint widths and depths. For the SC wall-to-wall joints, the joint area (A_j) is calculated as the total cross sectional area of the concrete infill within the joint region subjected to horizontal or vertical shear.

$$V_n = \gamma \sqrt{f_c'} A_j \tag{1}$$

OBJECTIVE AND EXPERIMENTAL APPROACH

The objective of this research is to evaluate the applicability and conservatism of the ACI 349-06 Section 21.5.3 RC beam-column joint shear strength equation with γ value equal to 12 for estimating the joint shear strength of SC wall T-joints. This paper presents the results of preliminary experimental and analytical investigations on this topic. Additional research is ongoing, and comprehensive results will be presented in a future forum and publication.

The preliminary experimental and analytical investigation was conducted on a large-scale SC wall T-joint. The specimen was designed to undergo joint shear failure instead of plasticity in the SC walls, which was achieved by thickening the steel plates to increase the flexural capacity of the connected SC walls. Table 1 shows geometry and material properties of SC wall-to-wall joints considered in this study. As shown in the table, Gr 50 steel was used for both steel faceplates and steel tie bars and 4000 psi normal weight concrete was used. The length of the connected SC walls were determined based on study

for the correlation between bending moment and shear force and the corresponding joint shear force. The length was determined such that the joint shear failure governs.

Table 1: Geometry and material properties of SC wall-to-wall T joints

Study	Geometry				Material Property					
	h, in.	*l*, in.	T, in.	t_p, in.	Concrete Infill, psi	Faceplates		Tie bars		Studs
						F_y, ksi	F_u, ksi	F_y, ksi	F_u, ksi	F_u, ksi
Experiment	60	60	30	0.75	6,473	58.6	83.9	60.4	69.1	74.0

Figure 3 shows the test setup for conducting the SC wall T-joint test. As shown, the setup is similar to that for an exterior beam-to-column joint test. The lateral loading (H) is applied at the top, and the specimen has pin and roller boundary conditions at the bottom and to the right. The figure also shows how the lateral load (H) is transferred to the support along with the bending moments and shear forces in the members.

High shear forces are generated in the joint region as illustrated in Figure 4. These are identified as the joint shear force in the continuous wall direction (V_{jc}) and joint shear force in the discontinuous wall direction (V_{jd}). These two joint shear force terms (V_{jc} and V_{jd}) are the resultants of: (i) the shear forces (H and R_y) acting on the joint surfaces, and (ii) the decomposed tension and compression forces from the bending moments acting on each side. In the figure, T is the overall depth of SC walls and j is the distance between the resultant compression force and tension force due to bending moments. The force equilibrium equation developed by Varma et al. (2011) for the cracked-transformed flexural section can be used to calculate j, however, its value is very close to 0.9 for all practical purposes. The two joint shear terms (V_{jc} and V_{jd}) are calculated as shown in Equations 2 and 3. V_{jc} is always larger than V_{jd} and used in the evaluation of the joint shear strength of SC wall to wall joints.

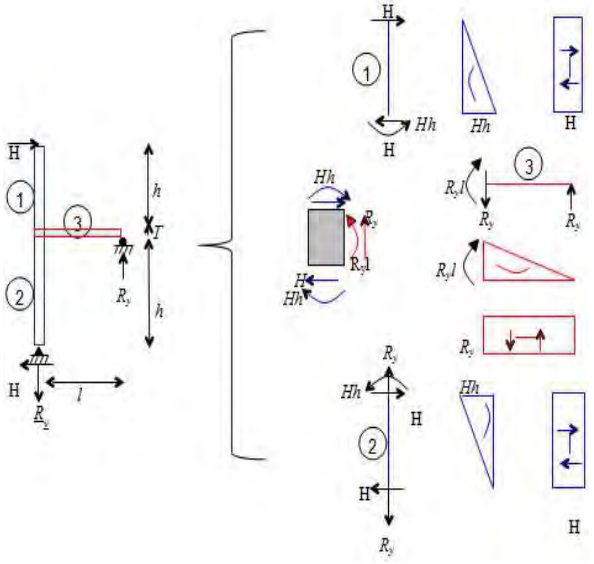

Figure 3 – Force transfer mechanisms

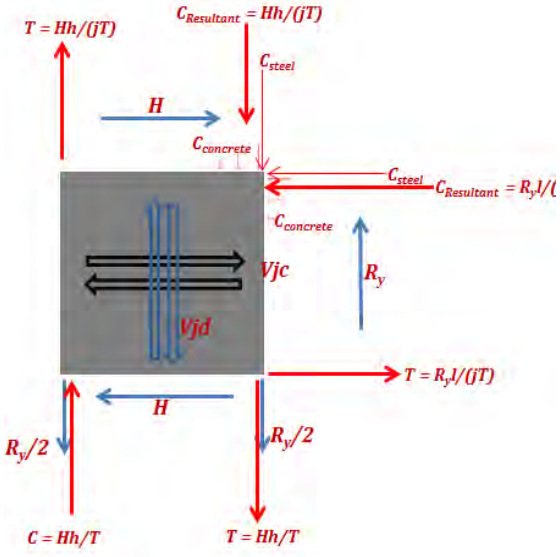

Figure 4 – Force transfer mechanisms focused in the joint region

$$V_{jc} = H - \frac{R_y l}{jT} \tag{2}$$

$$V_{jd} = -\left(\frac{Hh}{jT} - \frac{R_y}{2} + \frac{Hh}{T} \right) \tag{3}$$

PRE-TEST ANALYSIS RESULTS

The SC wall T-joint specimen was modeled with a commercially available 3D finite element analysis program, ABAQUS, to predict the joint shear behavior and joint shear strength. The concrete infill, steel tie bars, and steel faceplates were modeled using eight-node solid elements with reduced integration (C3D8R). The steel headed shear studs were modeled using beam elements (Quadratic Timoshenko beam elements).

The interfacial shear transfer mechanism between concrete infill and steel faceplate was modeled using connector elements. The empirical force slip equation derived by Ollgaard et al. (1971), as shown in Equations 4 and 5, was used to obtain shear stud capacity by specifying the diameter of the stud, ultimate strength of the steel and the concrete compressive strength. The shear stud connector elements are defined between coinciding steel and concrete nodes at shear stud locations.

Table 2 summarizes the geometric and material properties used for the analysis. As shown, expected material properties for both steel (F_y = 55 ksi) and concrete (f'_c = 6500 psi) were used in the study. The idealized uniaxial stress-strain (σ-ε) curve for steel was used for the analysis. The parameters used to define the idealized stress-strain curve consist of: (i) elastic modulus E, (ii) yield stress σ_y, (iii) yield strain ε_y, (iv) yield plateau length m, (v) strain corresponding to onset of strain hardening ε_{sh}, (vi) ultimate stress σ_u, and (vii) strain corresponding to ultimate stress ε_u.

Table 2: Assumed geometry and material properties of SC wall T-joint pre-test analysis

Study	Geometry				Material Property					
	h, in.	*l*, in.	T, in.	t_p, in.	Concrete Infill, psi	Faceplates		Tie bars		Studs
						F_y, ksi	F_u, ksi	F_y, ksi	F_u, ksi	F_u, ksi
Analysis	60	60	30	0.75	6,500	62.5	73.0	62.5	73.0	65.0

The concrete elastic fracture CEF model in ABAQUS was used to represent the complex behavior of concrete in tension and shear. The CEF model assumes elastic behavior in compression. In tension, it uses a brittle fracture model with oriented damaged elasticity concepts to model smeared cracking. It has anisotropic damage rules, and can be used with dynamic explicit analyses. The elastic modulus, Poisson's ratio, and uniaxial tension stress-crack opening displacement behavior need to be specified to adequately define the concrete models. The uniaxial tension strength and the post-peak behavior are defined using the equations for plain concrete provided in CEB-FIP-2010.

$$Q = Q_u(1 - e^{-18\Delta})^{2/5} \tag{4}$$

$$Q_u = \min(A_{stud}F_{u,stud}, 0.5A_{stud}\sqrt{f'_c E_c}) \tag{5}$$

The finite element analysis results showed a linear response after initial cracking almost up to the peak load. Concrete finite elements underwent significant deformation and high compressive stress were observed until yielding of tie bars in the discontinuous SC wall. The joint shear-displacement curve at the loading point predicted by the finite element analysis is shown in Figure 5. As seen in the figure, the specimen joint shear reached about 429 kips which is about 4 % greater than the joint shear strength (413 kips) calculated using the ACI 349-06 equation. The analytically predicted joint shear (panel shear)-shear deformation curve is shown in Figure 6. The stiffness gradually decreased as the load level increased and concrete finite elements cracked. Failure was characterized by yielding of the tie bar located in the concrete infill of the joint region followed by compression strut failure of the concrete.

Figure 7 (a) shows maximum principal strain contour plots of the concrete at the ultimate joint shear force. Maximum principal strains greater than 0.003 are shown in gray. Extensive cracking is observed in the joint region. Figure 7 (b) shows the minimum principal stress contour plots of the concrete. Minimum principal stresses less than -6500 psi are shown in black. Figure 7 (c) shows the equivalent plastic strain (PEEQ) contour in the steel faceplates. Any color other than blue indicates yielding. Yielding of the tie bar finite elements was observed.

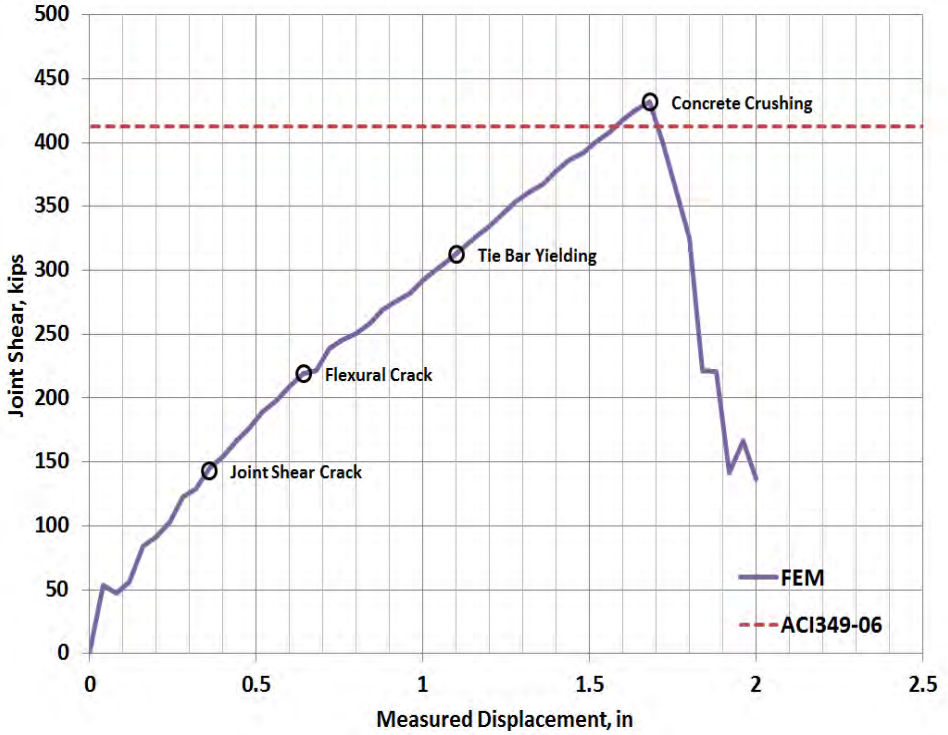

Figure 5 – Joint shear vs. displacement at loading point from pre-test analysis

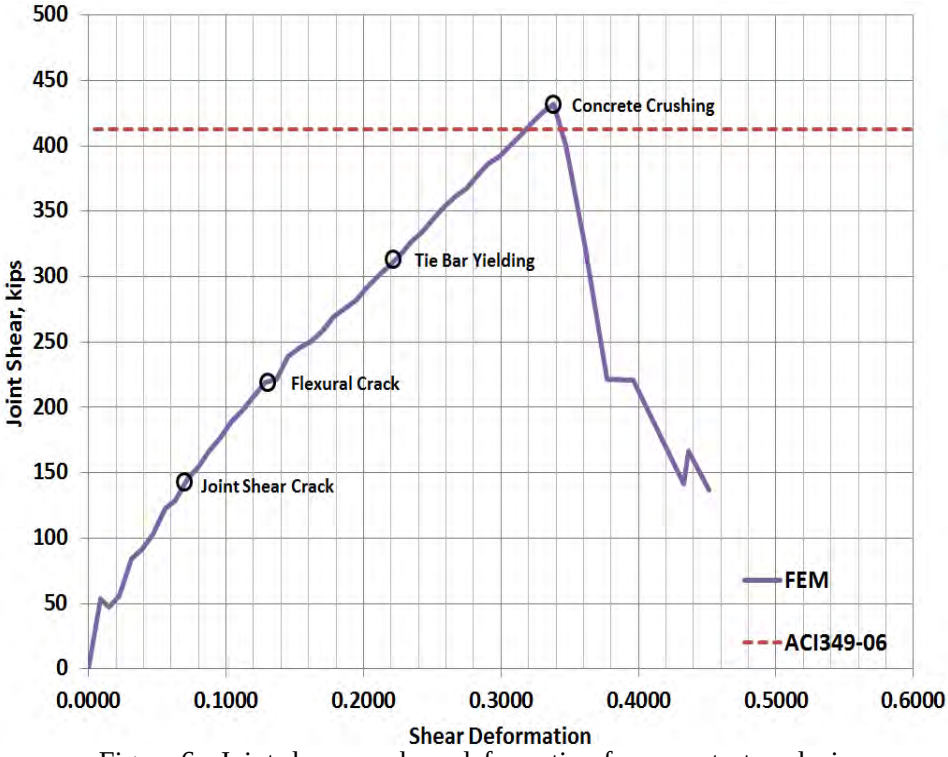

Figure 6 - Joint shear vs. shear deformation from pre-test analysis

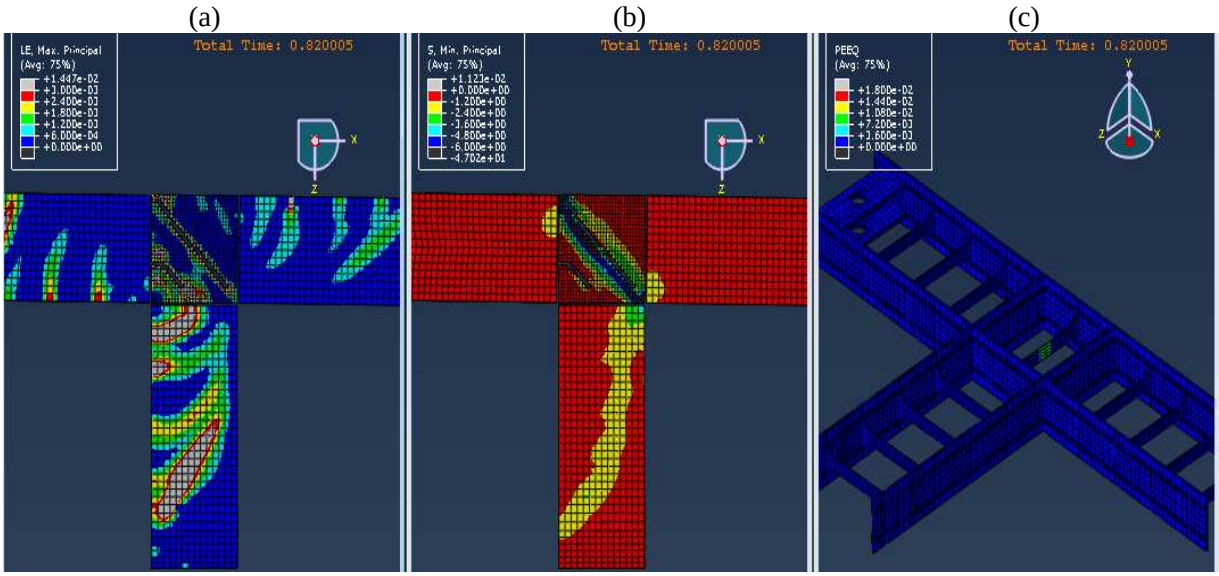

Figure 7 – Maximum principal strain distribution in concrete, (b) – Minimum principal stress distribution in concrete, and (c) – PEEQ distribution in steel faceplates and tie bars at ultimate joint shear force

EXPERIMENTAL RESULTS

The SC wall T-joint test was conducted using the test setup shown in Figure 8. As shown in Figure 8(a) and (b), the test specimen was subjected to lateral load (H) with pin and roller boundary conditions. The east end was supported by a rigid link with physical pins at each end that permit rotation as well as sliding (translation) in the east-west direction, but prevent displacement in the south-north direction. The distance between the east end and the joint surface is referred as *l*. The south end was supported using a steel rod that prevents translation in the north-south and east-west directions, but permits rotation to occur. The distance between the south end and the joint surface is referred as *h*. The lateral load (H) was applied to the north end of the specimen.

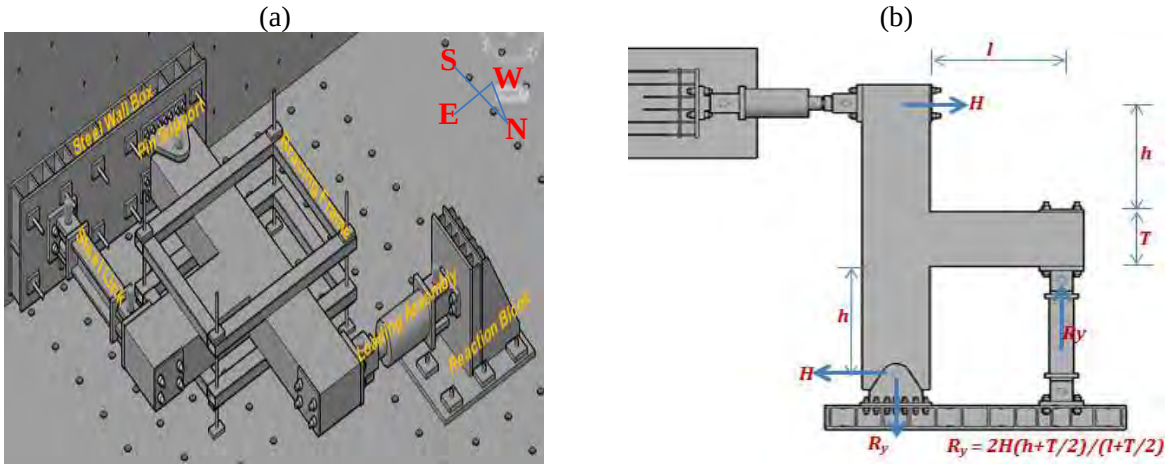

Figure 8 – Joint shear test schematic sketch: (a) isometric view and (b) plan view

The test consisted of four load cycles as stated below. V_n^{exp} is the expected shear force at the joint shear failure.

i. Load specimen to 30 kips – unload – -30 kips (2 Cycles) ($0.25V_n^{exp}$)
ii. Load specimen to 60 kips – unload – -60 kips (2 Cycles) ($0.50V_n^{exp}$)
iii. Load specimen to 90 kips – unload – -90 kips (2 Cycles) ($0.75V_n^{exp}$)
iv. Load specimen to 130 kips – unload– -130 kips (3 Cycles) ($1.05V_n^{exp}$)

Figure 9 shows the layout of the displacement sensors for the test specimen. Displacement transducers were attached to the test specimen to measure displacement in both North-South direction and East-West direction. Figure 10 shows the joint shear versus displacement relation from the specimen (SP1). The figure indicates a nearly elastic response up to 300 kips (75% of the expected load level at the joint shear failure mode). The stiffness of the specimen started to degrade during the last cycle, and was unloaded after its joint shear strength had been reached. As shown in Figure 10, the joint shear strength of the specimen exceeded both: (i) the joint shear strength calculated using ACI 349-06 equation, and (ii) the joint shear strength predicted by the pre-test analysis. Additionally, Figure 10 shows good comparison between the joint shear behavior predicted analytically and measured experimentally.

Figure 11(a) shows a photo of crack formation in the joint region at the failure taken during the experiment. The analytically predicted crack formation in the joint at the ultimate joint shear force is shown in Figure 11(b) for the comparison. As shown, the experimental crack formation in the joint region matches favorably with the predicted crack formation.

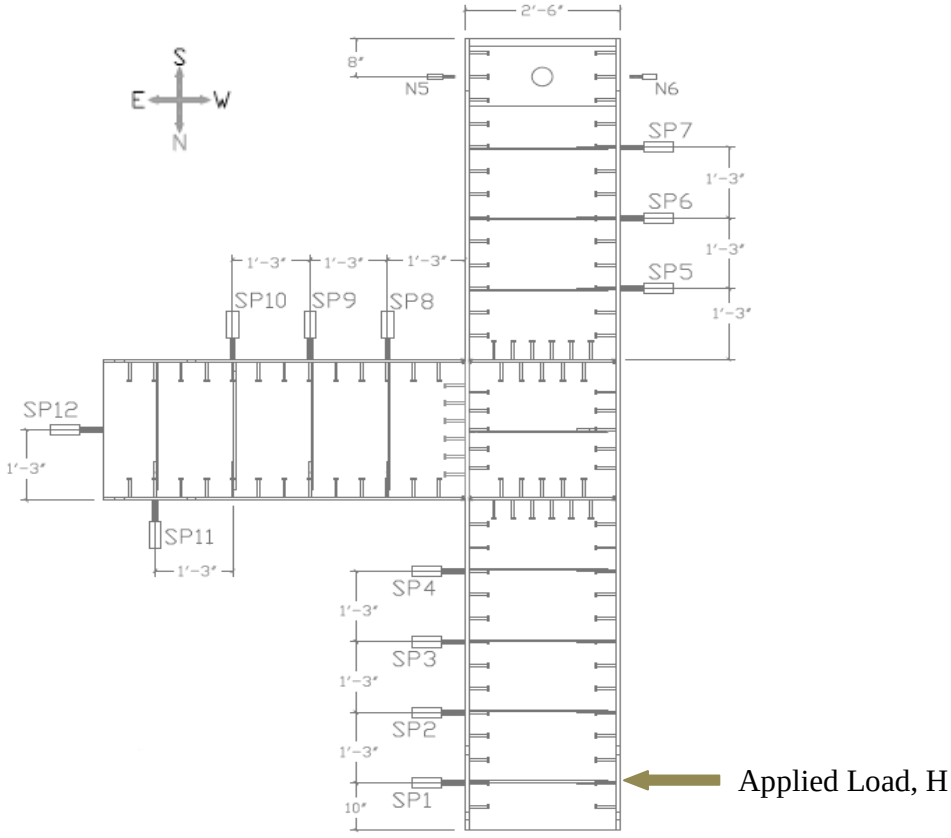

Figure 9 – Displacement sensor layout

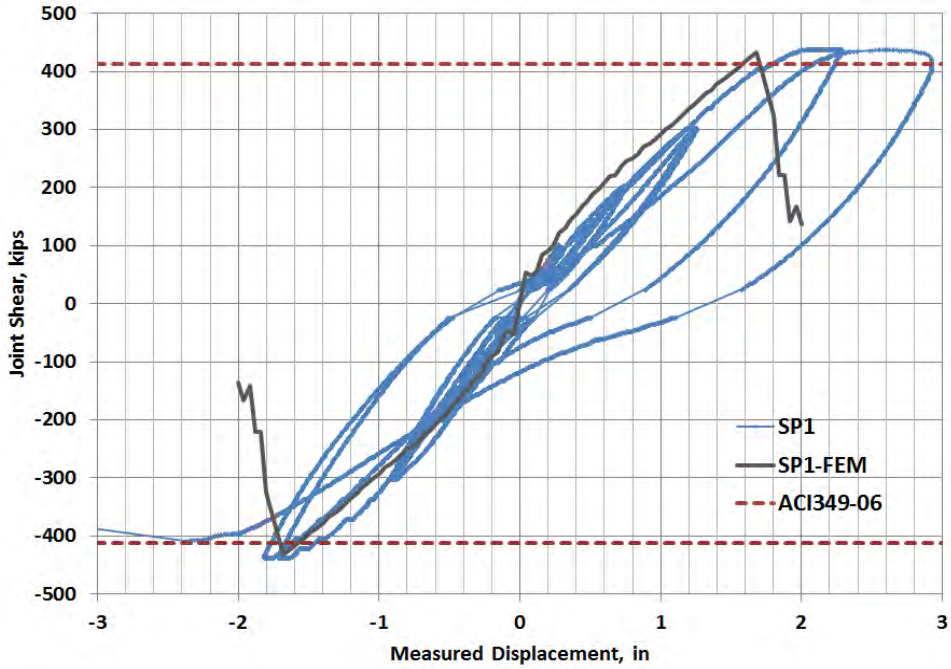

Figure 10 – Joint shear vs. deflection relations in the east-west direction for Specimen SP1

(a) (b)

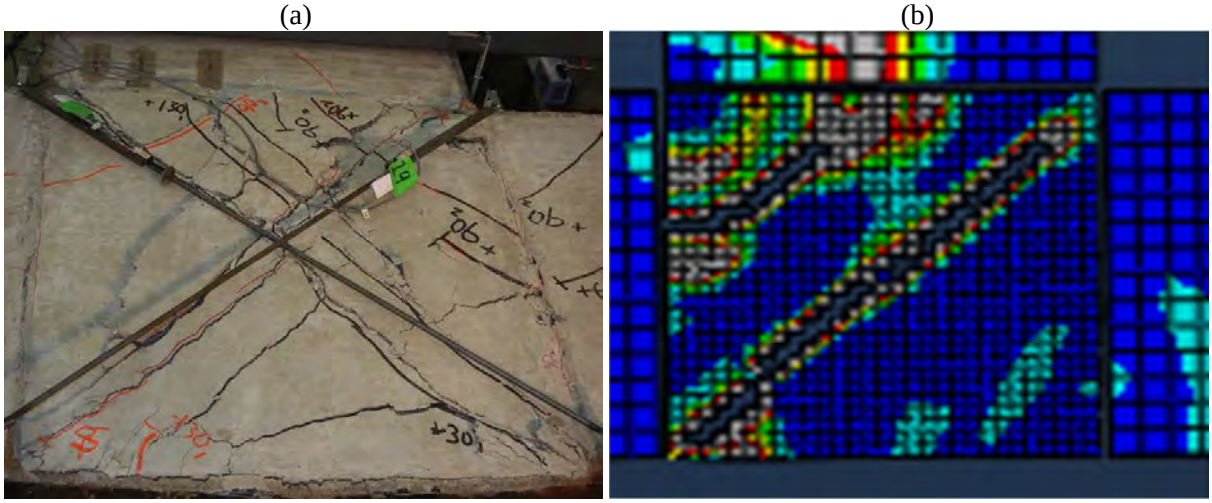

Figure 11 –Crack occurrence in the joint region at joint failure: (a) experiment and (b) FE analysis

CONCLUSIONS

Full-strength connection design is recommended for SC wall-to-wall T-joints, where energy dissipation occurs through inelasticity and formation of plastic hinges in the SC walls, and the joint region has adequate shear strength to resist the demands placed on it by the plastic hinges in the connected SC walls. However, limited information is available to asses the shear strength of SC wall T-joints. Therefore, in the absence of better information, the joint shear strength of reinforced concrete (RC) beam-to-column joints was considered for the SC wall T-joints.

Preliminary experimental and analytical investigations were conducted to evaluate: (i) the joint shear behavior and strength of SC wall-to-wall T joints, and (ii) the applicability and conservatism of the ACI 349-06 Section 21.5.3 RC beam-column joint shear strength equation with γ value equal to 12 for estimating the joint shear strength of SC wall T-joints.

This paper presented the results of the preliminary investigations on this topic including a large-scale test of an SC wall T-joint designed to fail in joint shear. The joint shear strength of the specimen exceeded both: (i) the joint shear strength calculated using ACI 349-06 equation, and (ii) the joint shear strength predicted by the pre-test analysis. Additionally, the joint shear behavior predicted analytically compared favorably with the experimental results. Additional research is ongoing and comprehensive results will be presented in a future forum and publication.

REFERENCES

KEPIC-SNG (2010). *Specification for Safety-Related Steel Plate Concrete Structures for Nuclear Facilities.* Board of KEPIC Policy, Structural Committee, Korea Electric Association

Varma, A.H., Seo, J., Chi, H., and Baker, T. (2011a). "Behavior of SC Wall Lap Splice Anchorages." Transactions of the 21st SMiRT Conference, New Delhi, India, Paper ID 765, IASMiRT, North Carolina State University, Raleigh, NC, USA

Varma, A.H., Malushte, S.R., Sener, K.C., Booth, P.N., Coogler, K. (2011b) "Steel-Plate Composite (SC) Walls: Analysis and Design Including Thermal Effects", Trans. of the Internal Assoc. for Struct. Mech. in Reactor Tech. Conf., SMiRT-21, Paper No. 761, New Delhi, India

ACI 349 (2006). "Code Requirements for Nuclear Safety-Related Concrete Structures and Commentary," American Concrete Institute, Farmington Hills, MI

ABAQUS (2011). *ABAQUS/Standard Version 6.10 User's Manuals: Volume I-III*, Hibbitt, Karlsson, and Sorenson Inc., Pawtucket, RI.

Ollgaard, J.G., Slutter, R.G., and Fisher, J.W. (1971) "Shear Strength of Stud Connectors in Lightweight and Normal-weight Concrete", Engineering Journal – American Institute of Steel Construction, Inc.

Model Code 2010, "First Complete Draft", fib bulletins 55 and 56, International Federation for Structural Concrete (fib), ISBN 978-2-88394-095-6 and ISBN 978-2- 88394-096-3

Joint ACI-ASCE Committee 352. (2002). "Recommendations for Design of Beam-Column Joints in Monolithic Reinforced Concrete Structures (ACI 352R-02)," American Concrete Institute, Farmington Hills, Mich.